RSC primes the quiescent genome for hypertranscription upon cell cycle re-entry

Christine E. Cucinotta, Rachel H. Dell, Keean C.A. Braceros, and Toshio Tsukiyama*

Division of Basic Sciences, Fred Hutchinson Cancer Research Center, Seattle WA

*To whom correspondence should be addressed.

Tel: 206-667-4996

Email: ttsukiya@fredhutch.org

Abstract

Quiescence is a reversible G_0 state essential for differentiation, regeneration, stem cell renewal, and immune cell activation. Necessary for long-term survival, quiescent chromatin is compact, hypoacetylated, and transcriptionally inactive. How transcription activates upon cell-cycle re-entry is undefined. Here we report robust, widespread transcription within the first minutes of quiescence exit. During quiescence, the chromatin-remodeling enzyme RSC was already bound to the genes induced upon quiescence exit. RSC depletion caused severe quiescence exit defects: a global decrease in RNA polymerase II (Pol II) loading, Pol II accumulation at transcription start sites, initiation from ectopic upstream loci, and aberrant antisense transcription. These phenomena were due to a combination of highly robust Pol II transcription and severe chromatin defects in the promoter regions and gene bodies. Together, these results uncovered multiple mechanisms by which RSC facilitates initiation and maintenance of large-scale, rapid gene expression despite a globally repressive chromatin state.

Introduction

For decades scientists have used budding yeast to uncover mechanisms of chromatin regulation of gene expression; and the vast majority of these studies were performed in exponentially growing (hereafter log) cultures [1]. Log phase, however, is not a common growth stage in unicellular organism lifecycles. Furthermore, many cell populations in multicellular organisms, such as in humans, are not actively dividing [2–4]. Indeed, the majority of “healthy” cells on Earth are not sustained in a persistently dividing state [3]. Non-proliferating cells reside in a G_0 state, which generally means these cells are either

terminally differentiated, senescent, or quiescent. The quiescent state provides advantages to organisms: quiescence allows cells to remain dormant for long periods of time to survive harsh conditions or to prevent over-proliferation [3–5,2]. Notwithstanding this so-called “dormant state”, quiescent cells can exit quiescence and re-enter the mitotic cell-cycle in response to growth cues or environmental stimuli, which distinguishes quiescence from other G_0 states. A major hallmark of quiescence is the chromatin landscape—vast histone de-acetylation and chromatin compaction occur during quiescence entry [6,7]. These events happen alongside a global narrowing of nucleosome depleted regions (NDR) and increased resistance to micrococcal nuclease (MNase) digestion, indicating a repressive chromatin environment [6]. Together, these features of quiescent cells point to a critical role for chromatin regulation of the quiescent state. However, the role of chromatin regulation upon exit from quiescence is unknown.

Reversibility is a conserved hallmark of quiescent cells and is required for proper stem-cell niche maintenance, T-cell activation, and wound healing in metazoans [4,8]. Therefore, we sought to elucidate molecular mechanisms by which cells can overcome this repressive chromatin environment to re-enter the mitotic cell cycle. Given its genetic tractability, the ease by which quiescent cells can be purified, and high level of conservation among chromatin and transcription machinery, we turned to the budding yeast *Saccharomyces cerevisiae* [9]. We can easily isolate quiescent yeast cells after seven days of growth and density-gradient centrifugation. In this context, we can study pure populations of quiescent yeast, a cell fate that is distinct from other cell types present in a saturated culture [10].

Since DNA is wrapped around an octamer of histone proteins in increments of ~147bp to form nucleosomes [11], enzymes must move nucleosomes to give access to transcription initiation factors [12]. One such enzyme is the SWI/SNF-family member, RSC, which is a 17-subunit chromatin remodeling enzyme complex [13]. RSC contains an ATP-dependent translocase, Sth1 [14–17], multiple subunits with bromodomains (more than half of all bromodomains in the yeast genome are in RSC) and two zinc-finger DNA-binding domains, which allow RSC to target and remodel chromatin [18,19]. Many components of the RSC complex are essential for viability in budding yeast and the complex is conserved in humans, where it is named PBAF. In humans, mutations in PBAF genes are associated with 40% of kidney cancers [20]; and 20% of all human cancers contain mutations within SWI/SNF family genes [21], underscoring the importance of such complexes in human health.

The best-described role for RSC in regulating chromatin architecture and transcriptions is its ability to generate NDRs, by sliding or evicting nucleosomes [22–24]. Moving the +1 nucleosome allows for TATA binding protein (TBP) promoter binding and transcription initiation [25]. To this end, RSC mostly localizes to the -1, +1, and +2 nucleosomes in log cells [26–28]. However, RSC has also been implicated in the transcription elongation step where it tethers to RNA polymerase and can localize to gene bodies [29–31]. Additionally, RSC binds nucleosomes within the so-called “wide NDRs”, where there are MNase-sensitive nucleosome-sized fragments, known as “fragile” nucleosomes [32–35]. These RSC-bound nucleosomes are likely partially unwrapped to aid in rapid gene induction [35–38].

69 In this study, we investigated how genes are transcribed during the first minutes
70 of quiescence exit. We were particularly interested in uncovering mechanisms to
71 overcome highly repressive chromatin found in quiescent cells. Unexpectedly, ~60% of
72 the yeast genome was transcribed by RNA polymerase II (Pol II) by the first 10-minutes
73 of exit, despite the highly repressive chromatin architecture present in quiescence. We
74 found that this hypertranscription [39] event is RSC dependent and that RSC binds
75 across the genome to ~80% of NDRs in quiescent cells. Upon RSC depletion, we
76 observed canonical abrogation of transcription initiation, defects in Pol II clearance past
77 the +1 nucleosome, and gross Pol II mislocalization, resulting in abnormal upstream
78 initiation and aberrant non-coding antisense transcripts. We further showed that RSC
79 alters chromatin structure to facilitate these processes. Taken together, we propose a
80 model in which RSC is bound to NDRs in quiescent cells to facilitate robust and
81 accurate burst of transcription upon quiescent exit through multiple mechanisms.
82

83 **Results**

84 **Hypertranscription occurs within minutes of nutrient repletion post-quiescence**

85 To determine the earliest time at which transcription reactivates during
86 quiescence exit, we fed purified quiescent cells YPD medium and took time points to
87 determine the kinetics of Pol II C-terminal domain (CTD) phosphorylation by western
88 blot analysis (Fig. 1A). Unexpectedly, Pol II CTD phosphorylation occurred within three
89 minutes (Fig. 1A, compare lanes 1 and 2), which was our physical limit of isolating cells
90 during this time course. To determine which transcripts were generated during these
91 early quiescence exit events, we performed nascent RNA-seq using 4-thio-uracil (4tU)

92 to metabolically label new transcripts [40,41]. In agreement with the western-blot
93 analysis, we observed a high level of transcriptional activation within a few minutes of
94 nutrient repletion (Fig. 1B). Based on our western-blot result, the highest Pol II CTD
95 phosphorylation is observed ~ten minutes after refeeding. Consistent with this result, we
96 observed the highest level of nascent transcripts at the ten-minute time point, where
97 ~1000 mRNAs (20% of the genome) were statistically significantly increased compared
98 to the zero-minute time point (Fig.1B, Fig.1—supplement 1A). Given how quickly Pol II
99 was phosphorylated and transcripts were generated, we sought to determine if high
100 levels of Pol II were already bound to the early exit genes in the quiescent state, as was
101 observed previously in a heterogenous population of stationary phase cells [42]. To this
102 end, we performed spike-in-normalized ChIP-seq analysis of Pol II in quiescent cells
103 and at several time points following refeeding (Fig. 1C, Fig. 1—supplement 1B). Low
104 Pol II occupancy levels (compare heatmaps 1 and 5) were detected in quiescent cells,
105 which agrees with our western blot and RNA-seq analyses and previously published
106 literature [6,43,7]. This implied that Pol II is not paused (Fig. 1C, compare heatmaps 1
107 and 2) in quiescent cells, and suggested that Pol II needs to be recruited *de novo* for
108 rapid initiation and elongation. In support of this conclusion, we detected only low levels
109 of the pre-initiation complex subunit TFIIB bound to genes in quiescent cells, which
110 increased ~3-fold by five minutes of exit (Fig. 1—supplement 1C).
111 Highlighting the high level of transcription occurring in the first ten minutes of
112 quiescence exit, we observed a drop-off in Pol II occupancy levels around the first G2/M
113 phase (240 minutes) (Fig. 1C-D, Fig. 1—supplement 1D). Indeed, when the data were
114 sorted into k-means clusters across the time course, we noticed that many of the genes

115 expressed in the 240-minute time point were similar, but still not identical, to those
116 expressed in log cells, suggesting a recovery to log-like gene expression profile takes
117 hours post refeeding (Fig. 1C, compare columns 4 and 5, Fig. 1D). There was a ~1.7-
118 fold increase in overall Pol II occupancy in the 10-minute time point relative to that of log
119 cells (Fig. 1D, Fig.1—supplement 1B). Together, these results demonstrate transcription
120 activates extremely rapidly and robustly in response to nutrient repletion.
121

122 **Chromatin bears hallmarks of repression during early quiescent exit time points**

123 Given the exceptionally high transcriptional response during the first ten minutes of
124 quiescence exit, we wondered whether chromatin changes reflected hypertranscription.
125 To this end, we performed ChIP-seq analysis of H3 to measure nucleosome occupancy
126 levels genome wide over time. Global H3 patterns during the early exit time points,
127 especially at the 5-minute time point, were more similar to that of the quiescent state
128 than to the 240-minute time point (Fig. 2A, compare columns 1-3), despite higher
129 transcription levels. The most striking changes in histone occupancy during the early
130 time-points were within NDRs, where the pattern at the 10-minute timepoint resembles
131 the 240-minute time point (Fig. 2A, B). However, the H3 profiles outside of NDRs (Fig.
132 2A, compare column 1-3 and 4 to the right of NDR, and Fig.2B) remain similar to that of
133 quiescent state during the early stage of quiescent exit. In addition to nucleosome
134 occupancy, we tested nucleosome positioning using MNase-seq analysis where
135 nucleosomes with 80% of the digested chromatin is represented by mononucleosomes.
136 Globally, nucleosome positions were stable across the early exit time points (Fig. 2C).

137 We next tested if a burst of histone acetylation occurred during these early exit
138 time points to help overcome the repressive quiescent chromatin environment. To test
139 this, we performed ChIP-seq analysis of H4ac using an antibody that recognizes penta-
140 acetylated H4. Similar to nucleosome occupancy and positions, a modest increase in
141 histone H4 acetylation occurred, but the levels did not reflect that of log cells (Fig. 2D,
142 E). This suggests that, while there was a strong transcriptional response during
143 refeeding, histone acetylation was delayed. This result is in agreement with a recent
144 study demonstrating that histone acetylation takes place mostly as a consequence of
145 transcription [44].
146 To assess a biological readout of the repressive chromatin environment, we
147 turned to phenotypic analysis of TFIIS disruption. TFIIS is a general elongation factor
148 that rescues stalled Pol II; and nucleosomal barriers have been shown to increase
149 stalled Pol II [45]. Given that Pol II stalling is common across the genome [46], it is
150 paradoxical that the gene encoding TFIIS is not essential for viability in actively dividing
151 cells, and its deletion does not cause strong growth defects [47]. Since Pol II must
152 achieve a high level of transcription in the repressive chromatin environment during
153 early quiescence exit, we hypothesized that TFIIS may play more critical roles during
154 this period than during log culture. Indeed, in the absence of TFIIS (*dst1*Δ), quiescent
155 yeast cells exhibited defects in cell cycle re-entry, where cells lacking TFIIS stall at the
156 first G1 during exit, which is not the case during the mitotic cell cycle (Fig. 2F, Fig. 2—
157 supplement 1B). These results collectively revealed that the chromatin environment
158 remains repressive during early quiescence exit.
159

160 **In quiescence, RSC re-localizes to NDRs of genes expressed in exit**

161 Given the modest changes in chromatin at most genes during the early stage of
162 quiescence exit (Fig. 2), we wondered whether MNase-sensitive or "fragile"
163 nucleosomes were present at the promoters of rapidly induced genes in quiescence and
164 were removed in early exit. Thus, we performed a weaker (low) MNase digestion (10%
165 mononucleosomes) (Fig. 3A) and compared it to the stronger (high) MNase digestion
166 (80% mononucleosomes) (Fig. 3B). Supporting our hypothesis, comparing the weaker
167 MNase digest to the stronger MNase digest revealed that ~1000 genes have fragile
168 nucleosomes in quiescent cells, which are reduced during exit (Fig. 3A). Additionally,
169 we noticed that the MNase-sensitivity of the +1 and +2 nucleosomes increased at the
170 10-minute time point, likely coinciding with transcription.

171 It has been recently suggested that that the ATP-dependent chromatin remodeler
172 RSC can remove fragile nucleosomes from promoters to activate transcription [25].
173 Additionally, it was proposed that RSC-bound nucleosomes are remodeling
174 intermediates that render such nucleosomes more MNase-sensitive [37]. Thus, RSC
175 was a strong candidate for regulating rapid transcription activation during quiescence
176 exit. We performed ChIP-seq analysis of the RSC catalytic subunit Sth1 in quiescent
177 cells. In quiescence, Sth1 exhibited a striking difference in binding pattern compared to
178 log cells (Fig. 3C, D). Sth1 bound to ~80% of NDRs at gene promoters in quiescent
179 cells (Fig. 3E, Figure 3—supplement 1A). This result was distinct from log cells, where
180 RSC was reported to occupy the widest NDRs but otherwise bind the -1, +1, and +2
181 nucleosomes for most highly expressed genes (Fig. 3C) [27,25,37]. The RSC binding
182 pattern in quiescent cells instead mirrored a recently described binding pattern in heat

183 shock, where RSC and other transcription regulators *transiently* relocate to the NDRs
184 [48]. In contrast to the heat shock response, however, we observed a stable, strong
185 binding pattern of RSC in NDRs regardless of NDR width (Fig. 3E). Another obvious
186 distinction of RSC binding patterns between log and quiescence was observed at tRNA
187 genes (Fig. 3F). RSC's role at tRNA expression has been well-studied in log cells [49–
188 51]. In quiescence, RSC was occluded from tRNAs genes. Whereas upon exit, RSC
189 rapidly targeted tRNAs, mimicking the log pattern. Together these data suggest that
190 RSC adopts a quiescence-specific binding profile, one in which RSC is bound to NDRs
191 more broadly across the genome.
192 We next sought to gain insight into how quiescent RSC occupancy patterns
193 might predict Pol II occupancy during exit. To this end, we compared localization of
194 RSC and Pol II in quiescence and exit. We first found that the presence of RSC at
195 NDRs in quiescent cells and strong transcription in exiting cells co-localized (Fig. 3—
196 supplement 1A). Next, we examined RSC occupancy changes during quiescence exit at
197 Pol II-transcribed genes. During quiescence exit, RSC began to move out of NDRs and
198 into gene bodies as transcription increased (Fig. 3G). These results suggested that
199 RSC facilitates transcriptional activation upon exit and raised the possibility that RSC
200 binding in NDRs may be a mechanism for cells to prepare for quiescence exit.
201
202 **RSC depletion causes quiescent exit defects and global Pol II occupancy**
203 **reduction during quiescence exit**
204 To test the requirement of RSC in quiescence exit, we simultaneously depleted two
205 essential subunits of the RSC complex, Sth1 and Sfh1, using the auxin degron system

206 [52], during quiescence entry (see methods; Figure 3—supplement 1B). Depletion of
207 these subunits throughout the exit process (hereafter "-RSC") caused a dramatic defect
208 in cell cycle progression upon quiescence exit, where the cells exhibited strong delays
209 in exiting the first G1 stage (Figure 4A). This result contrasted with that in cycling cells,
210 where *rsc* mutants or conditional alleles cause G2/M arrest [53].

211 To determine the impact of RSC depletion on hypertranscription during
212 quiescence exit, we performed Pol II ChIP-seq analysis on cells exiting quiescence. In
213 the presence of RSC, Pol II levels peaked at 10 minutes and substantially decreased at
214 30 minutes after the exit (Fig. 4B, compare columns 3 and 4). As is the case in log
215 cultures [49,54,55], Pol II occupancy decreased in the absence of an intact RSC
216 complex in Q-cells and upon nutrient repletion thereafter (Fig. 4B). Pol II occupancy did
217 eventually increase over time in the RSC-depleted samples. However, even after 30-
218 minutes, Pol II did not reach the peak level of occupancy seen at the 10-minute mark in
219 the +RSC condition (Fig. 4B, compare heatmaps 3 and 8, and 4C). This suggests that
220 the defect in Pol II occupancy during quiescence exit was not solely due to slower
221 kinetics.

222 As shown earlier in Figure 3G, we observed RSC leaving the NDRs and moving
223 into gene bodies during quiescence exit. Therefore, we examined the impact of RSC
224 depletion on nucleosome occupancy and positioning. H3 ChIP-seq showed that RSC is
225 required for removal of histones within NDRs (Fig. 4D), which is consistent with RSC's
226 role as the "NDR creator" [23]. Together, these data provide mechanistic explanations
227 for how RSC facilitates Pol II loading during early stages of quiescence exit.
228

229 **RSC is required for Pol II passage through gene bodies**

230 Given that RSC moves from NDRs into gene bodies during quiescence exit (Fig. 3G),
231 we next tested whether RSC could aid transcription after initiation. To this end, we
232 selected ~2000 genes where RSC moved toward gene bodies and examined RSC
233 localization at the 10-minute time point of quiescent exit. This analysis showed uniform
234 movement of RSC from NDR into gene bodies (Fig. 5A). We next tested whether this
235 RSC movement is dependent on Pol II transcription. To this end, we performed Sth1
236 ChIP-seq analyses during quiescence exit in the presence of a transcription inhibitor
237 1,10-phenanthroline (Fig. 5B, Pol II control in Fig. 5—supplement 1A). This experiment
238 demonstrated that the movement of RSC from NDRs into gene bodies was strongly
239 inhibited by 1,10-phenanthroline, establishing that RSC re-localization during quiescent
240 exit is dependent on Pol II transcription.

241 Co-transcriptional movement of RSC into gene bodies suggested a possibility
242 that RSC may help Pol II passage through gene bodies. To test this, we determined the
243 effects of RSC depletion on Pol II localization during early time points of quiescent exit.
244 Fig. 5C and D show that RSC depletion affects Pol II localization in at least two ways
245 during early quiescent exit. First, consistent with Fig 4B, the robust increase in the
246 amount of Pol II over genes is strongly decreased upon RSC depletion. In addition,
247 upon RSC depletion, Pol II sharply accumulates at TSSs at the 5-minute mark, which
248 continued to the 10-minute mark. In sharp contrast, Pol II accumulates at slightly more
249 downstream at the 5-minute mark and moves mostly to downstream regions at the 10-
250 minute time point in the presence of RSC. We also noticed a pile-up of Pol II at the 3'-
251 end of genes at the 5-minute timepoint upon RSC depletion (Fig. 5C). This is in

252 agreement with the possibility that RSC may be involved in proper transcription
253 termination [56]. At these loci, NDRs are relatively shallow in quiescence but histone
254 density rapidly decreases upon quiescence exit in the presence of RSC (Fig. 5E, Fig.
255 5—supplement 1B). In the absence of RSC at these sites, however, histone density is
256 unexpectedly lower at NDR in quiescence but does not change during quiescent exit
257 (Fig. 5F, Fig. 5—supplement 1B), suggesting defective chromatin structure at and
258 downstream of the NDR. Together, these results are consistent with the notion that co-
259 transcriptional movement of RSC facilitates passage of Pol II through nucleosomes
260 immediately downstream of TSSs through chromatin regulation.
261

262 **RSC suppresses abnormal upstream transcription initiation**

263 The fact that Pol II accumulated upstream of TSSs at the 5-minute mark upon RSC
264 depletion (Fig. 5C) suggested possible defects in transcription start site selection. To
265 test this possibility, we examined the 4tU-seq profiles of a subset of RSC targets (1426
266 genes) in which there appeared to be an enrichment of RNA signal directly upstream
267 and downstream of TSSs. We took the $\log_2$ ratio of RNA signal in the depleted condition
268 versus the non-depleted condition at the ten-minute time point (Fig. 6A). We sorted the
269 genes using k-means clusters and took into account RSC binding when determining
270 gene sets to analyze.

271 This analysis revealed that upon RSC depletion a large number of genes (~1400)
272 exhibited increased nascent sense-strand RNA signals starting upstream of their normal
273 TSSs, demonstrating wide-spread defects in TSS selection. Examination of individual
274 loci revealed that, in addition to filling of an NDR at the normal TSSs, an NDR is created

upstream, which overlaps with ectopic transcription observed at an upstream TSS (see Fig. 6B for an example). These results suggest that RSC facilitates selection of accurate transcription initiation sites through proper NDR formation upstream of protein coding genes during the burst of transcription during quiescence exit. This is likely a quiescence-specific function of RSC, or a result of the robust hypertranscription event during exit, as depletion of Sth1 in cycling cells mostly repressed transcription initiation with relatively few new upstream transcription start sites [54,55].

RSC is required for suppression of anti-sense transcripts during quiescence exit

Given the robust transcriptional response during the early minutes of quiescence exit (Fig. 1), we examined whether aberrant transcripts might also arise during quiescence exit when RSC was depleted. Indeed, in many cases we found antisense transcripts arising in the absence of RSC. We found ~900 RSC targets that had generally reduced sense transcript levels with strongly upregulated cognate antisense transcripts (Class I), and ~600 genes (Class II) with only modest changes in both sense and anti-sense transcript levels upon RSC depletion (Fig. 7A). Chromatin analyses of individual Class I loci revealed that RSC depletion caused narrower NDRs upstream of the sense TSS (see Fig. 7B for an example). In contrast, NDRs for sense transcripts remained largely open at Class II genes (Fig. 7B). Both classes have RSC bound at the promoters of the sense genes in quiescence, with slightly higher RSC binding in the class I genes (Fig. 7C). Strikingly, nucleosome positioning was heavily impacted in the Class I set of genes upon RSC depletion in the sense direction, where NDRs became more resistant to MNase and nucleosomes in gene bodies were shifted toward the 5'-ends of genes. This

298 was in contrast to that of Class II where NDRs were largely open (Fig. 7D). Consistent
299 with the MNase-mapping data, nucleosome occupancy at NDRs and in gene bodies are
300 much more strongly affected by RSC depletion at Class I genes than Class II genes
301 (Fig. 7E). It is likely that Class II genes overcome the absence of RSC by having more
302 "fragile" nucleosomes that can be readily removed by general regulatory factors [25].
303 These results collectively showed that chromatin structure at the Class I genes is
304 especially dependent on RSC. In both classes of genes, RSC signals and RSC-
305 dependent chromatin changes are not apparent around the start sites of anti-sense
306 transcripts. Therefore, suppression of anti-sense transcripts is unlikely to be a direct role
307 for RSC. Instead, it is likely that both Class I and II genes, especially the former, have
308 an intrinsic property to allow anti-sense transcription to occur when not properly
309 regulated, and RSC is targeted to them to ensure sense transcription takes place
310 through formation of proper NDRs.
311

312 **Discussion**

313 In this report we have shown that there is a rapid and robust transcriptional response
314 during the very early minutes of quiescence exit (Fig. 8A). This response is greatly
315 dependent on the chromatin remodeling enzyme RSC. We found that RSC promotes
316 transcription at the right place and time in four different ways: 1) RSC promotes
317 transcription initiation by creating NDRs in quiescence and maintaining them during exit
318 (Fig. 8B). 2) RSC moves into gene bodies and helps Pol II transcribe past the +1
319 nucleosome (Fig. 8C). 3) RSC maintains proper NDR locations to allow for accurate
320 transcription start site selection (Fig. 8D). 4) RSC suppresses cryptic antisense

321 transcription via generating NDRs at the cognate sense genes (Fig. 8E). Together, our
322 results suggest that the massive transcriptional response requires highly accurate
323 nucleosome positioning to allow for cells to exit from the quiescent state.

324 Quiescent yeast must downregulate their transcriptional program and generate a
325 repressive chromatin environment in order to survive harsh conditions for extended time
326 periods [9,6,57,7,7,58]. How, then, do cells rapidly escape the quiescent state when
327 conditions are favorable? In this study, we show that there is an incredibly strong
328 transcriptional response to nutrient repletion after quiescence, notwithstanding a
329 relatively repressive chromatin environment that persists until the first G2/M phase after
330 quiescence. Indeed, we identified a previously unidentified phenotype for the deletion of
331 the gene encoding yeast TFIIS, *dst1*Δ. High numbers of stalled Pol II are present in
332 cycling cells [46] despite the little impact of deleting *DST1* on cycling cell growth. We
333 speculate cells exiting quiescence may rely more heavily on TFIIS to transcribe through
334 repressive chromatin [59,60].

335 During quiescence, RSC relocates to NDRs upstream of Pol II transcribed genes
336 that are transcribed in exit. Although RSC binds and regulates chromatin around Pol III
337 genes [26,49], RSC is depleted at tRNA genes in quiescence and only returns during
338 quiescence exit, further supporting the notion that RSC is globally re-targeted in
339 quiescence. This is distinct from the transient NDR-relocalization observed in heat
340 shock [48], as what we observed in quiescence was a sustained and rather stable
341 localization. How RSC binds to these new locations in quiescence is unknown. Given
342 the distinct structure of quiescent chromatin there are several, non-mutually exclusive,
343 explanations for RSC's binding pattern in quiescence. 1) The genome is hypoacetylated

344 and thus RSC can no longer bind to acetylated nucleosomes in quiescence via its
345 bromodomains [18]. However, given the highly robust response to refeeding, RSC
346 activity must be poised to be active in this state. An intriguing possibility could be that
347 histone acetylation inhibits RSC activity to some extent as was recently reported *in vitro*
348 [61]. This would be consistent with the rapid changes in nucleosome positioning at
349 many genes during quiescence exit in the absence of high levels of histone acetylation.
350 2) Recent structural studies have shown that the nucleosome acidic patch is in direct
351 contact with subunits of the RSC complex [62–65]. If the acidic patch is occluded by
352 hypoacetylated H4 tails in quiescence for example [11,66–69], it is possible that RSC
353 can no longer interact with this region of the nucleosome, rendering its binding abilities
354 different in quiescence. Finally, 3) a lack of Pol II activity in quiescent cells could prevent
355 RSC from moving out of NDRs and into gene bodies. Indeed, transcription appears to
356 play a prominent role in RSC localization: RSC moves into gene bodies during
357 transcription activation and this movement is blocked when transcription is inhibited, as
358 we have reported above. It is likely that a combination of transcription and histone
359 acetylation helps pull RSC into gene bodies, given recent work showing that acetylation
360 is a consequence of transcription [44]. In a separate study, we recently found that the
361 SWI/SNF remodeling enzyme promotes transcription of a subset of hypoacetylated
362 genes during quiescence entry, implying a specialized transcription regulation program
363 for essential genes in the wake of widespread transcriptional shutdown [57]. In cycling
364 cells, it was recently shown that RSC and SWI/SNF cooperate at a subset of genes
365 [70]. Our results suggested that cooperation between the two SWI/SNF class
366 remodeling factors may also occur during quiescence entry.

367 Consistent with co-transcriptional re-localization, our data suggest RSC plays an
368 active role in helping Pol II transcribe past the +1 nucleosome in addition to initiating
369 transcription. Supporting this idea was our observation of a subset of genes where RSC
370 depletion caused a Pol II enrichment around the +1 nucleosome. Previous reports
371 showed that RSC can bind gene bodies and impact elongating and terminating Pol II
372 [30,56]; and one study showed interactions between the Rsc4 subunit and all three RNA
373 polymerases [29]. An intriguing possibility could be that RSC directly interacts with Pol II
374 to facilitate transcription past the first few nucleosomes.
375 The transcriptional response during quiescent exit was dampened by depleting
376 the essential chromatin remodeler, RSC, but it did not diminish completely. Pol II
377 occupancy was globally decreased ~2-fold at the 10-minute time point in RSC-depleted
378 cells. However, at ~900 genes we found that while sense transcription was reduced,
379 antisense transcripts were generated. This was largely due to a nearby NDR
380 susceptible to transcription initiation that could be co-opted for antisense transcription.
381 The mechanism that allows for this cryptic transcription is still unknown. Chromatin
382 remodeling enzymes are vastly important for repressing antisense lncRNAs [71].
383 Different chromatin remodeling enzymes function to repress lncRNA transcripts in
384 cycling cells, including RSC [72,73]. We speculate RSC is particularly suitable to
385 regulate global transcriptome during quiescence exit due to its high abundance, which
386 allows it to function through multiple mechanisms. The mouse embryonic stem cell-
387 specific BAF complex was also recently shown to globally repress lncRNA expression
388 [74]. This raises the possibility that some of our observations in yeast quiescent cells
389 could be conserved in mammalian quiescent cells. Given the robust transcriptional

390 response that occurs during quiescence exit, it is likely that chromatin structure is
391 crucial for maintaining the quality of the transcriptome. Indeed, we noted cases where
392 transcription occurred upstream of the canonical TSS when an NDR was not generated,
393 highlighting the defects in Pol II initiation and start site selection due to chromatin
394 defects in the absence of RSC. Hypertranscription events similar to the one observed
395 during quiescence exit occur throughout all organisms, particularly during development
396 [39]. Therefore, it is quite possible that we will see similar, multifaceted roles for RSC
397 homologues or other abundant chromatin remodeling factors in facilitating proper
398 hypertranscription in many other systems.
399

400 **Materials and Methods**

401 **Yeast strains, yeast growth media, quiescent cell purification, and exit time**
402 **courses**

403 The *S. cerevisiae* strains used in this study are listed in Supplementary Table S1 and
404 are isogenic to the strain W303-1a with a correction for the mutant *rad5* allele in the
405 original W303-1a [75]. Yeast transformations were performed as previously described
406 [76]. All cells were grown in YPD medium (2% Bacto Peptone, 1% yeast extract, 2%
407 glucose). We note that quiescent (Q) yeast need to be grown in YPD using “fresh”
408 (within ~three months) yeast extract as a source. To purify Q cells, liquid YPD cultures
409 were inoculated with a single colony into liquid cultures (colonies were no older than
410 one week). Yeast were grown in Erlenmeyer flasks ten times the liquid volume for seven
411 days at 30°C and shaking at 180 RPM. Q cells were purified by percoll gradient
412 centrifugation as previously described [10]. Briefly, percoll was diluted 9:1 with 1.5 M

413 NaCl into 25-mL Kimble tubes and centrifuged at 10,000 RPM for 15-minutes at 4°C.
414 Seven-day cultures were pelleted, washed with ddH2O, resuspended in 1 mL of
415 ddH2O, and gently pipetted over a pre-mixed percoll gradient. 400 OD_{660} were pipetted
416 onto a 25-mL gradient. Gradients with loaded cells were centrifuged for one hour at
417 1000 RPM, 4°C. The upper, non-quiescent cell population and the middle, ~8 mL
418 fraction, were carefully discarded via pipetting. The remaining volume was washed
419 twice with ddH2O in a 50 mL conical tube at 3,000 RPM, 10 minutes each.
420 Q exit experiments were performed as follows: Q cells were harvested and
421 added to YPD to 1 OD_{660}/mL. Cells were grown at 25°C to slow the kinetics for
422 feasibility. For ChIP-seq and MNase-seq experiments, cells were grown to the
423 appropriate time and then crosslinked for 20 minutes (described in more detail in the
424 sections below).
425
426 **Depletion of RSC subunits, Sth1 and Sfh1**
427 The yeast strains YTT 7222 and 7224 were grown in 5-mL overnight YPD cultures, back
428 diluted for four doublings, and inoculated to 0.002 OD_{660} into the appropriate YPD
429 volume for a given experiment. Cells were grown for 16 hours and monitored for
430 glucose exhaustion using glucose strips. Six hours after glucose exhaustion, 1mg/mL of
431 Indole-3-acetic acid (Sigma, I3750-5G-A) was added, in powder form, to the culture. Q
432 cells were purified as described above and depletion efficiency was determined by
433 western blot analysis (Supplementary Figure 1A).
434
435 **Western Blot Analysis**

436 Yeast cells were lysed by bead beating in trichloroacetic acid (TCA), as previously
437 described [77]. Proteins were resolved on 8% polyacrylamide gels and transferred to
438 nitrocellulose membranes. Membranes were incubated with primary antibodies: anti-
439 Rpb3 (Biolegend, 665003 1:1000 dilution), anti-Ser5p (Active Motif, 61085 1:1000
440 dilution), anti-Ser2p (Active Motif, 61083, 1:1000 dilution), and anti-HSV (Sigma, 1:500).
441 Following primary incubation, membranes were incubated with either anti-mouse or
442 anti-rabbit secondary antibodies (Licor, 1:10000). Protein signals were visualized by the
443 Odyssey CLx scanner.
444
445 **ChIP-seq**
446 100 OD_{660} U of cells were crosslinked and sonicated in biological duplicate using the
447 protocol described in [78]. Proteins were immunoprecipated from 1 µg chromatin and 1
448 µL of anti-H3 (Abcam, 1791) conjugated to 20 µl protein G magnetic beads (Invitrogen,
449 10004D) per reaction. For Pol II ChIPs, we used an antibody against the Rpb3 subunit
450 (2 µl per reaction, Biolegend) conjugated to 20 µl protein G magnetic beads (Invitrogen,
451 10004D). For Sth1 ChIP experiments we used an antibody against the Flag-epitope tag,
452 FLAG M2 mouse monoclonal (Sigma Aldrich, F1804) and conjugated to 20 µl protein G
453 beads (Invitrogen, 10004D) Libraries were generated using the Ovation Ultralow v2 kit
454 (NuGEN/Tecan, 0344) and subjected to 50-bp single-end sequencing on an Illumina
455 HiSeq 2500 at the Fred Hutchinson Cancer Research Center genomics facility. We
456 used bowtie2 to align raw reads to the sacCer3 reference genome [79]. Reads were
457 then filtered using SAMtools [80]. Bigwig files of input-normalized ChIP-seq data were
458 generated from the filtered bam files using deepTools2 [81] and dividing the IP data by

459 the input data. Matrices for metaplots were generated in deepTools2 using the
460 annotation file from [82].
461
462 **MNase-seq**
463 Cell growth and crosslinking was done in the same fashion as in ChIP-seq experiments.
464 Generally, we followed the protocol in [78], with changes described here. Cells were
465 spheroplasted using 10 mg zymolyase (100T, AMSBIO, 120493-1) per 100 OD_{660} cells.
466 For Q cells, zymolyase treatment could take up to two hours. We monitored the cells via
467 microscopy and stopped the spheroplasting step when ~80% of the cells were
468 spheroplasted. MNase digestion was performed as described in [78]. High digests (80%
469 mononucleosomes) required 50U of micrococcal nuclease (Worthington, LS004798)
470 and for the low digests, chromatin was treated with 10 U of MNase. From this step,
471 chromatin was reverse crosslinked as described in [78]. Following reverse crosslinking,
472 RNase, and proteinase-K digestion, DNA was phenochloroform-extracted. Any large,
473 uncut genomic DNA species was separated out using Ampure beads (Beckman).
474 Sequencing libraries were generated from the purified DNA using the Ovation Ultralow
475 v2 kit (NuGEN, 0344). Libraries were subjected to 50-bp paired-end sequencing on an
476 Illumina HiSeq 2500 at the Fred Hutchinson Cancer Research Center genomics facility.
477 We used bowtie2 to align raw reads to the sacCer3 genome and filtered reads using
478 SAMtools as described above for ChIP-seq analysis. Bigwig files of input-normalized
479 ChIP-seq data were similarly generated from the filtered bam files using deepTools2
480 and the MNase option to center the reads around nucleosome dyads. Data represented
481 in the paper were filtered to mononucleosome sizes using deepTools2.

482

483 **Nascent RNA-seq**

484 Generally, nascent RNA-seq experiments were performed as described in
485 [83,41]. For the 0-minute and 5-minute samples, we added 100 and 50 OD_{660} of Q cells,
486 respectively, to YPD containing 5 mM 4-thiouracil (Sigma, 440736-1G). Cells were
487 incubated with 4tU for 5 minutes before pelleting (one minute, 3500 RPM) and flash
488 frozen in liquid nitrogen. For the 10-minute time points, 50 OD units of quiescent cells
489 were released into YPD for 5 minutes before an additional 5-minute incubation with 4tU
490 at a final concentration of 5 mM. All time points were labeled with 4tU for a total of 5
491 minutes before pelleting and freezing. Total RNA was isolated using Ambion's RiboPure
492 Yeast Kit (Thermo, AM1926). *S. cerevisiae cells* were lysed in the presence of
493 *Kluvomyces lactis* (*K. lactis*) cells in a 100:1 mixture. RNA was treated with DNAseI
494 according to the TURBO DNase kit (Thermo, AM2238). 40 ug RNA was then
495 biotinylated with MTSEA biotin-XX (diluted in 20% DMF) at a final concentration of 16.4
496 uM in 20mM HEPES pH 7.4 and 1 mM EDTA at room temperature for 30 minutes.
497 Unreacted MTS-biotin was removed from samples by PCI extraction and resuspended
498 in 100 uL nuclease-free water. Strepavidin beads (Invitrogen 65001) were washed with
499 high-salt wash buffer (100 mM Tris, 10 mM EDTA, 1 M NaCl, 0.05% Tween-20) and
500 blocked for one hour in high-salt wash buffer containing 40 ng/uL glycogen. 40 uL of
501 streptavidin beads were added to the RNA samples and incubated for 15 minutes at
502 room temperature. Beads were washed three times in 1 mL high salt wash buffer and
503 eluted for 15 minutes at room temperature in 50 uL streptavidin elution buffer (100 mM
504 DTT, 20 mM HEPES, 2.7, 1 mM EDTA, 100 mM NaCl, 0.05% Tween-20). The resulting

505 RNA was then purified and concentrated using the Qiagen miRNeasy kit (#217084).
506 Libraries were prepared from 5 ng of RNA using the Ovation SoLo kit (NuGEN/Tecan,
507 custom AnyDeplete; contact Tecan for ordering this kit for yeast). Libraries were
508 subjected to 50-bp paired-end sequencing on an Illumina HiSeq 2500 at the Fred
509 Hutchinson Cancer Research Center genomics facility. We used bowtie2 to align raw
510 reads to the sacCer3 and *K. lactis* (Ensembl ASM251v1) genomes and filtered reads
511 using SAMtools as described above for ChIP-seq analysis. Differential expression
512 analysis was performed using DESeq2 [84]
513

514 **Acknowledgements**

515 We are grateful to members of the Tsukiyama lab for helpful comments and critical
516 reading of this manuscript. We thank Sarah Hainer and Felix Mueller-Planitz for advice
517 on MNase-seq experiments. We thank Benjamin Martin, Rafal Donczew and Sandipan
518 Brahma for advice and feedback. We thank Mitchell Ellison and Alex Francette for
519 advice about analyzing nascent RNA-seq data. TT was supported by the National
520 Institutes of Health (R01 GM111428 and R35GM139429). CEC was supported by the
521 National Cancer Institute (T32CA009657) and National Institutes of Health
522 (F32GM131554).
523
524

525 **Declaration of Interests**

526 The authors declare no competing interests.

FIGURE 1

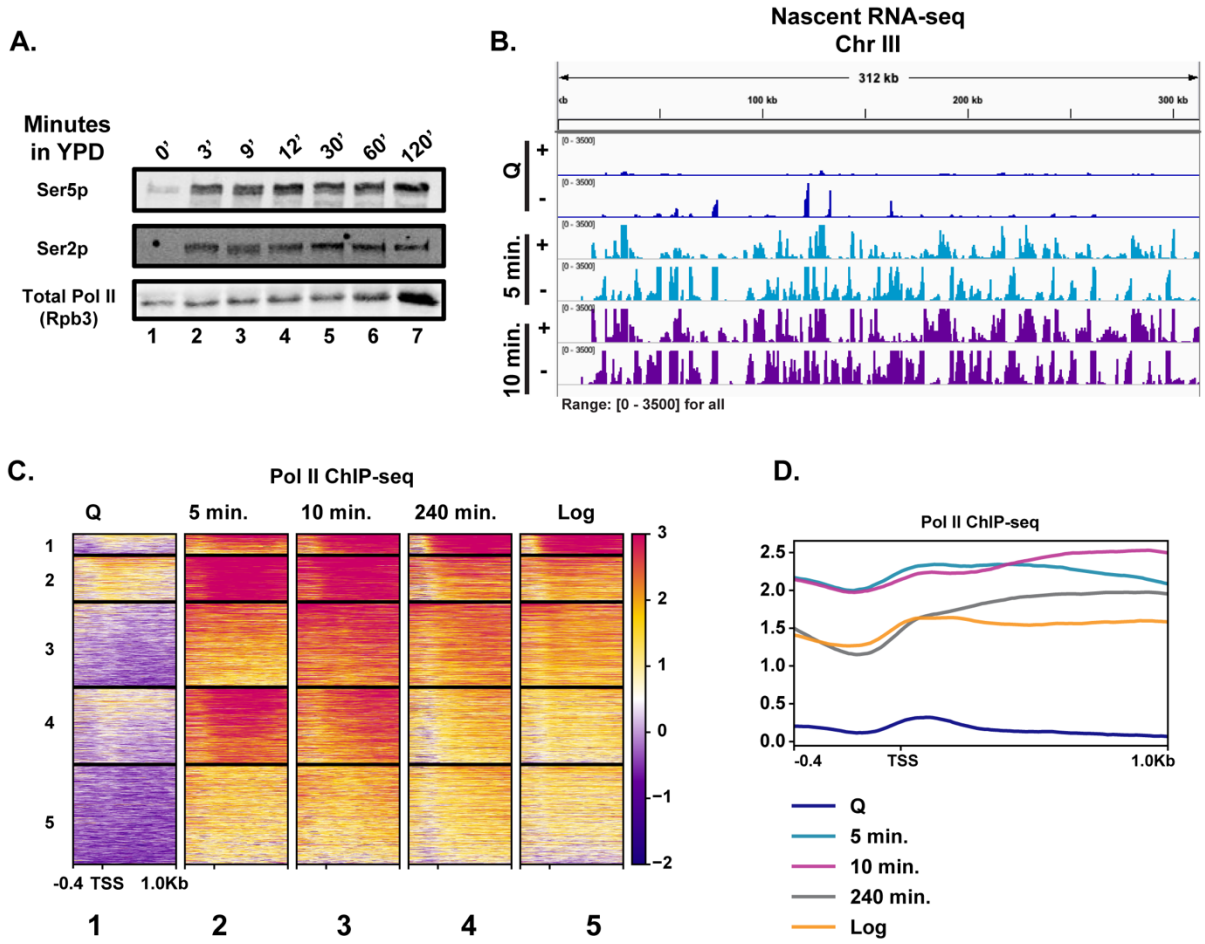

Figure 1. Rapid hypertranscription occurs upon nutrient repletion of quiescent cells

(A) Western blots were probed with antibodies to detect Ser5p and Ser2p of the CTD of Rpb1 subunit of Pol II. An antibody against the Rpb3 subunit of Pol II was used as a loading control. **(B)** Strand-specific 4tU-seq analysis. "+" indicates Watson strand and "-" indicates Click strand. **(C)** Pol II ChIP-seq analysis. Heatmaps show k-means clusters of 6030 genes. Genes are linked across the heatmaps. **(D)** Metaplots of ChIP-seq data shown in (C) without k-means clustering.

FIGURE 1—supplement 1

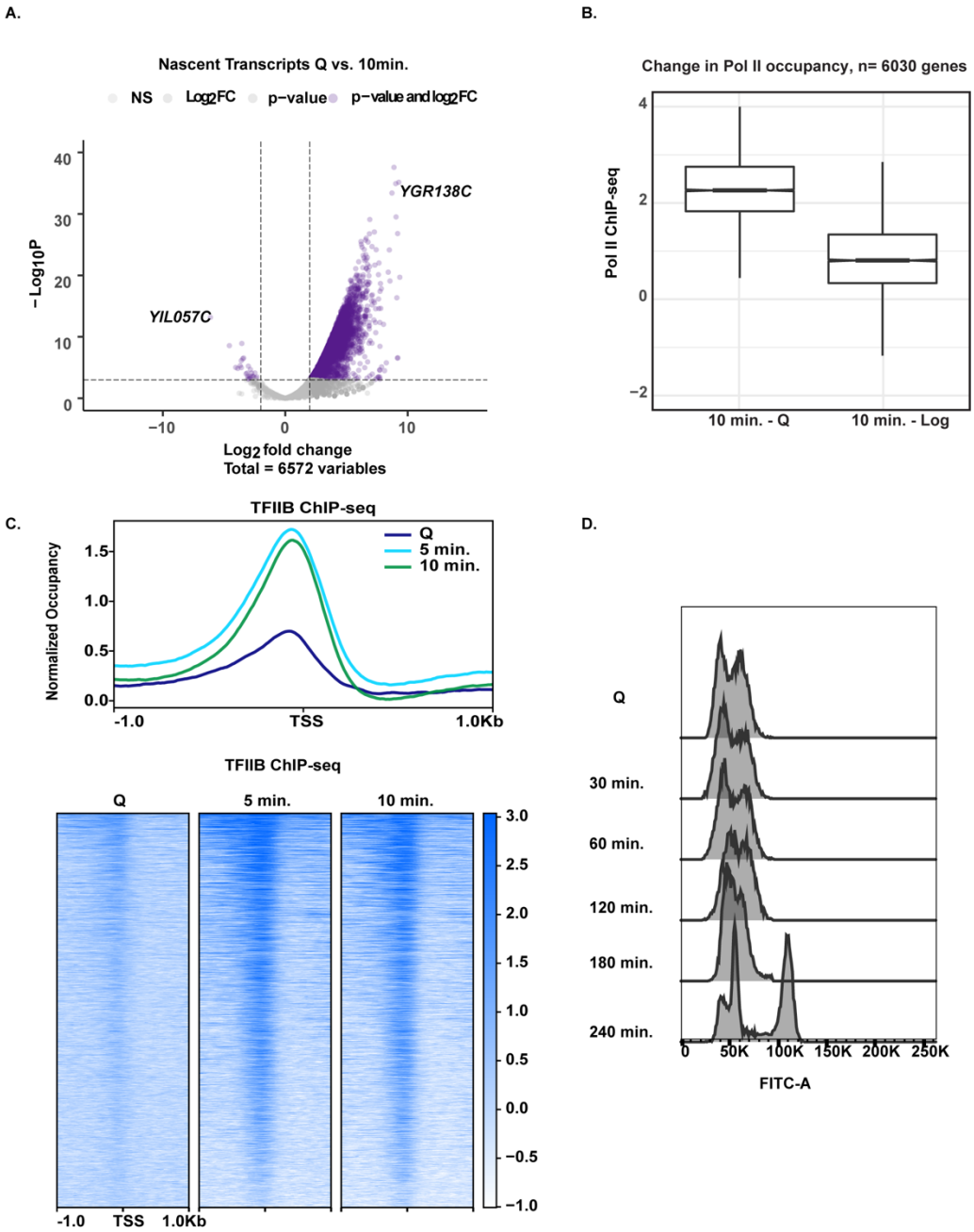

Figure 1—supplement 1
(A) Volcano plot of nascent transcripts comparing significant changes in expression using a 2-fold cut off. **(B)** Boxplots illustrating the difference in Pol II ChIP-seq signals across genes. Log_2 ratio values were subtracted (ex: Q log_2 values were subtracted from 10 min. log_2 values). **(C)** TFIIB ChIP-seq analysis in Q cells and exit time points. Genes are linked across the time points and are aligned to TSS. **(D)** DNA content FACS analysis indicating cell cycle progress during Q exit.

FIGURE 2

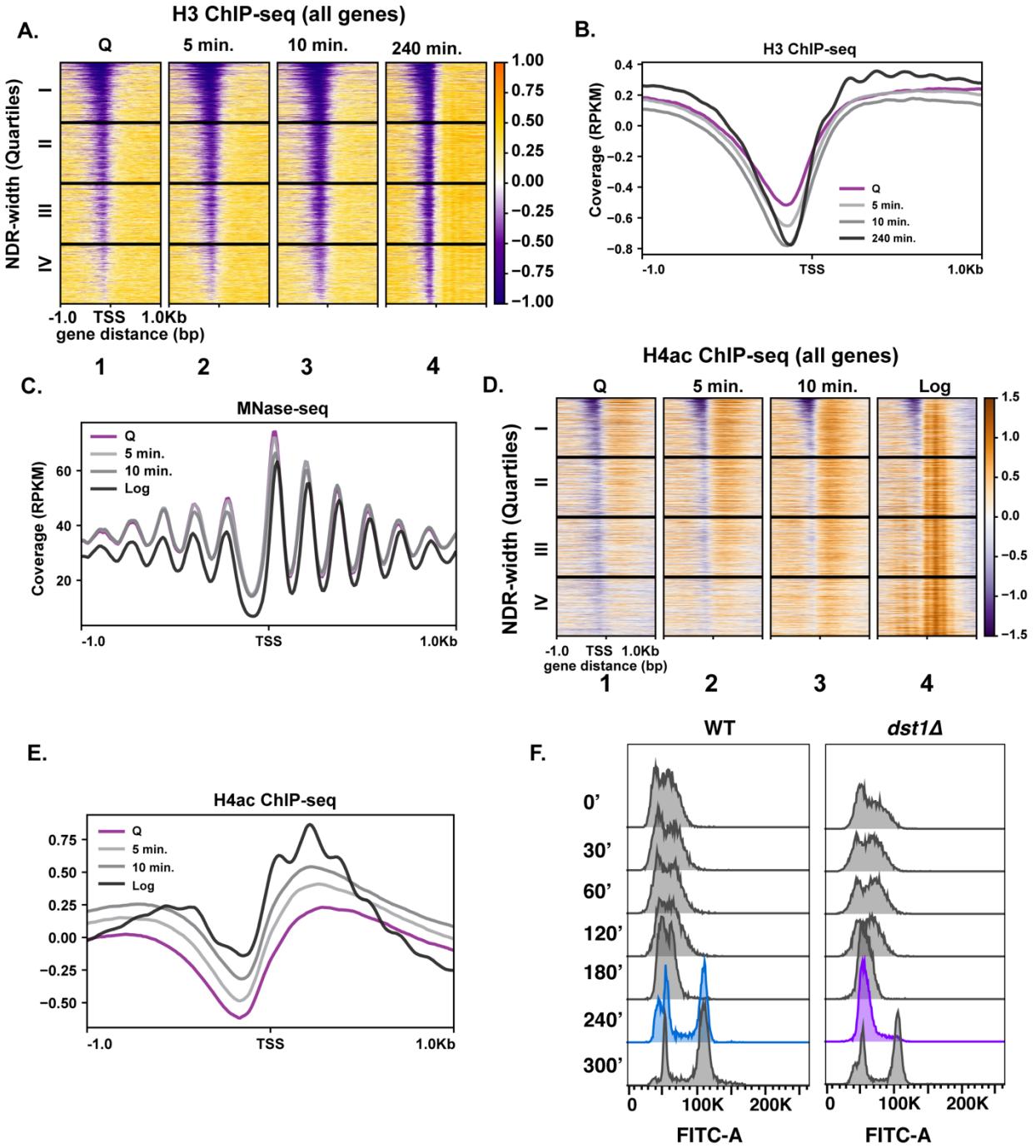

Figure 2. Repressive chromatin persists during early quiescence exit
(A, B) ChIP-seq of total H3 in quiescent cells and exit time points sorted into quartiles based on NDR width. **(C)** MNase-seq analysis of 6030 genes in Q (pink line), Log (black line), and Q-exit time points 5 minutes (light grey line) and 10 minutes (dark grey line). **(D, E)** ChIP-seq analysis of penta-acetylated H4 (H4ac) in Q and Log cells and exit time points. Genes are separated as in (B). **(F)** DNA content FACS analysis following Q exit in WT and a TFIIS-absent strain (*dst1*Δ).

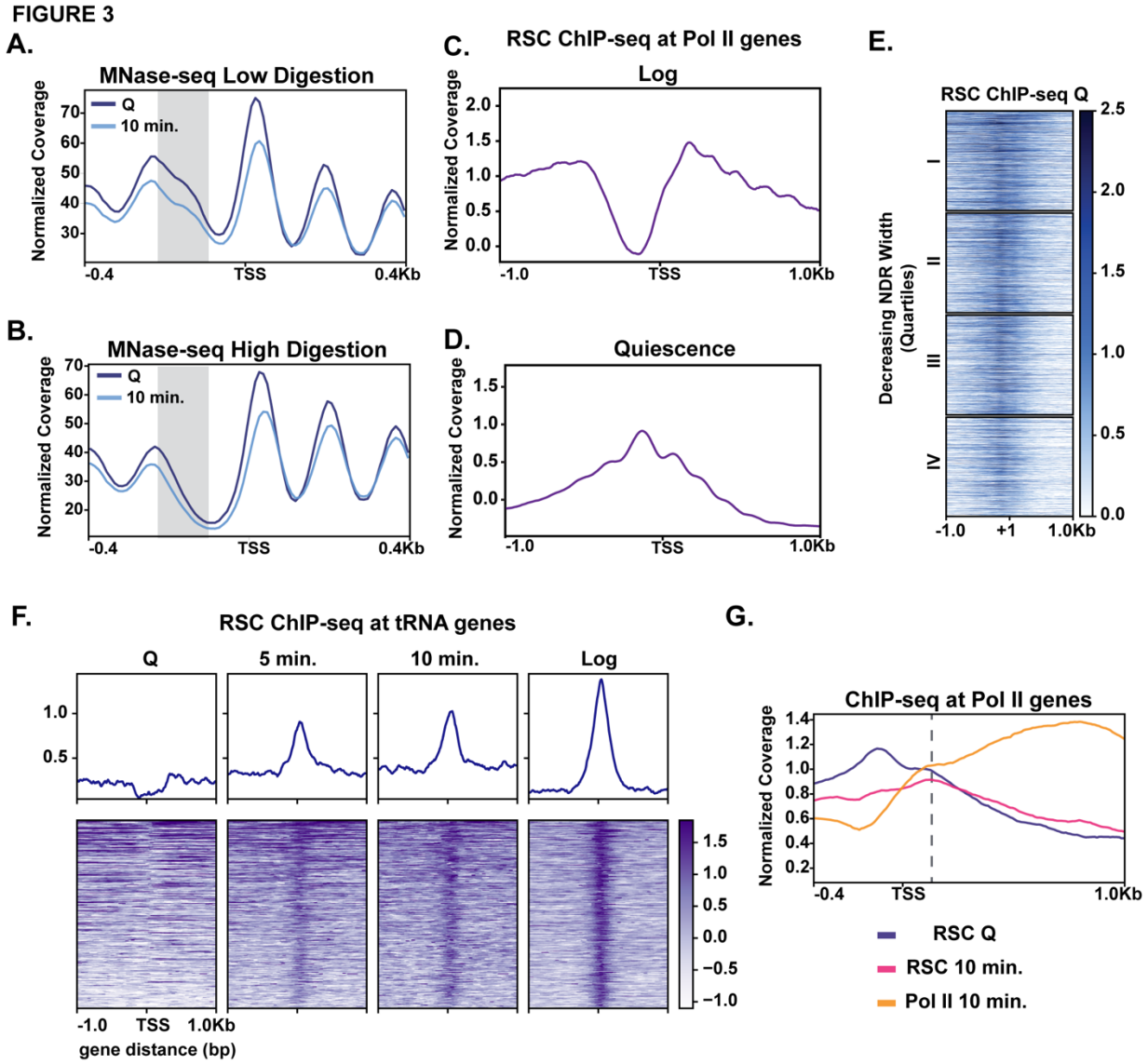

Figure 3. MNase sensitivity and quiescence-specific RSC relocalization indicate remodeling activity required for early exit

(A) MNase-digested chromatin to 10% mononucleosomes (low digestion). **(B)** Metaplot of MNase-digested chromatin to 80% mononucleosomes (high digestion) in Q and 10-minute time points. **(C,D)** ChIP-seq of the catalytic RSC subunit in quiescent and log cells at Pol II-transcribed genes. **(E)** ChIP-seq analysis of RSC shown across quartiles based on MNase-seq determined NDR width. **(F)** ChIP-seq of RSC at tRNA genes. **(G)** ChIP-seq of RSC and Pol II comparing RSC movement with Pol II into gene bodies.

FIGURE 3—supplement 1

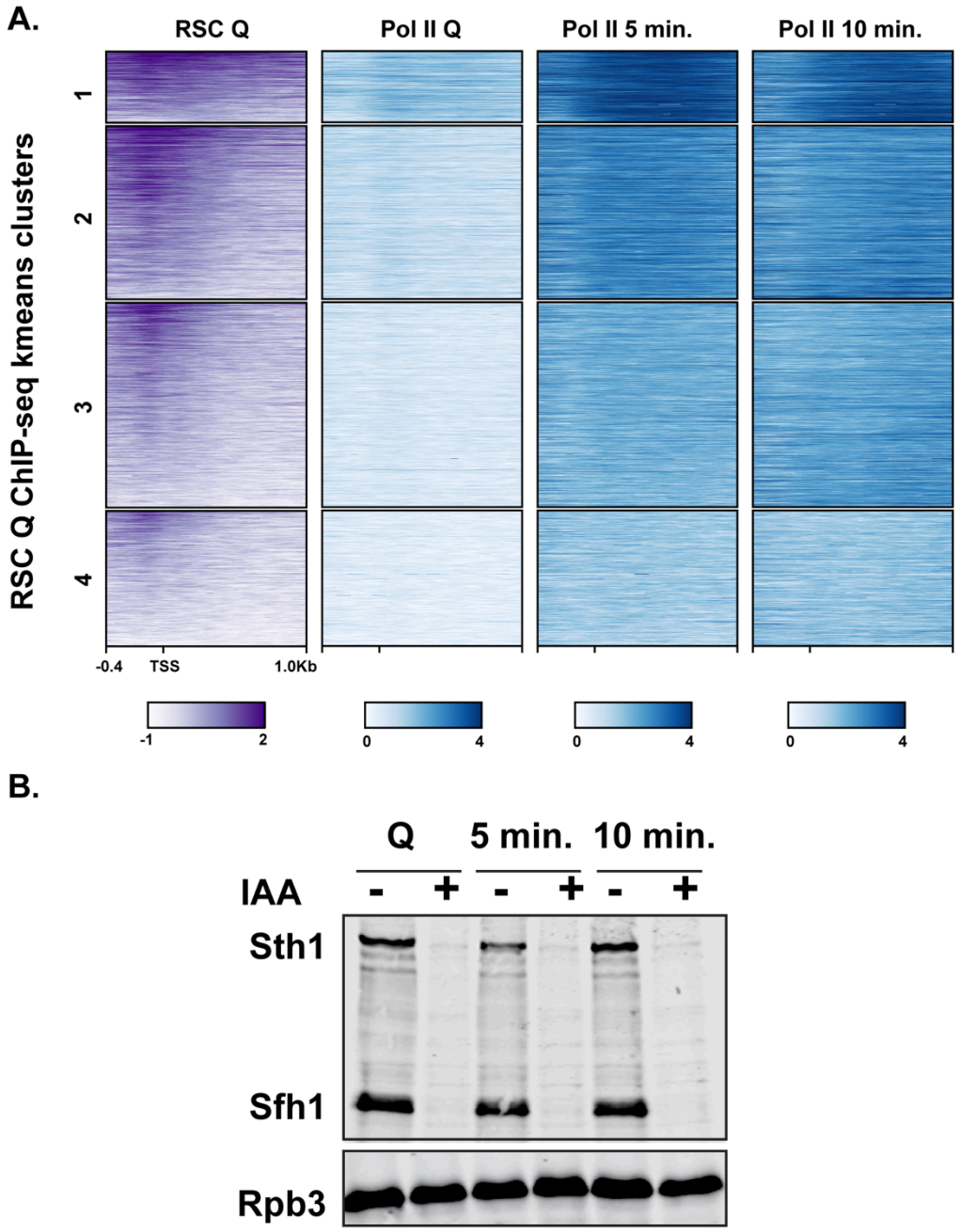

Figure 3—supplement 1
(A) ChIP-seq analysis of RSC and Pol II using antibodies against Flag-tagged Sth1 and Rpb3, respectively. Genes are sorted into k-means clustered and are linked across the different ChIPs. **(B)** Western blot analysis of RSC depletion. Both Sth1 and Sfh1 contain C-terminal HSV and AID tags for detection and depletion using IAA. Western blot was probed with an antibody recognizing the HSV epitope tag and Rpb3 (Pol II subunit) as a loading control. The addition of IAA is indicated by – or +.

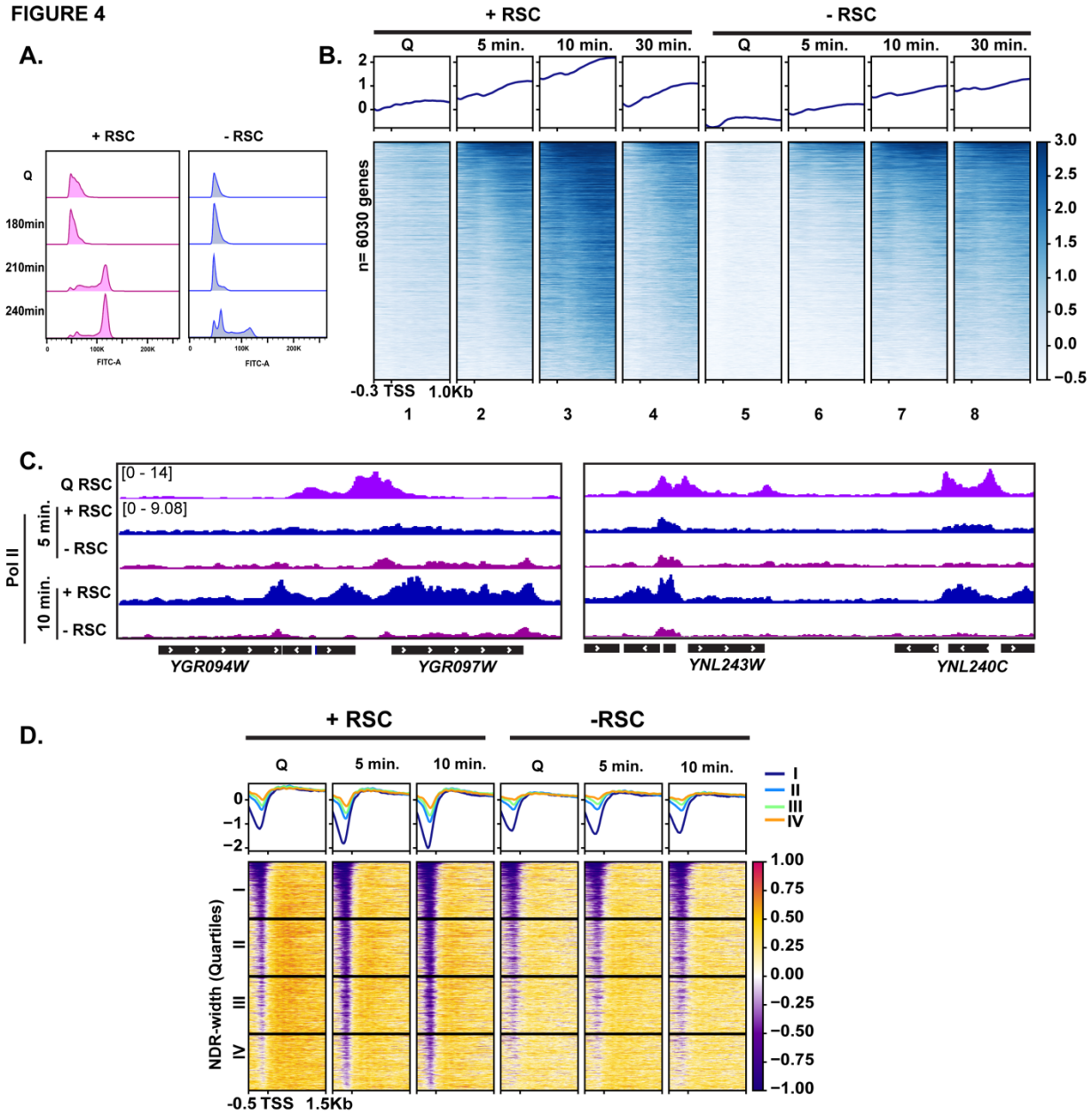

Figure 4. RSC is required for normal quiescence exit and hypertranscription upon nutrient repletion

(A) DNA content FACS analysis indicating cell cycle progression during Q exit in the presence (+) or absence (-) of RSC. **(B)** ChIP-seq analysis of Pol II across time in the presence or absence of RSC. Genes are sorted the same in all heatmaps. **(C)** Example tracks of data shown in **(B)** with RSC ChIP-seq in Q cells added. **(D)** H3 ChIP-seq sorted by NDR width (as determined by MNase-seq experiments).

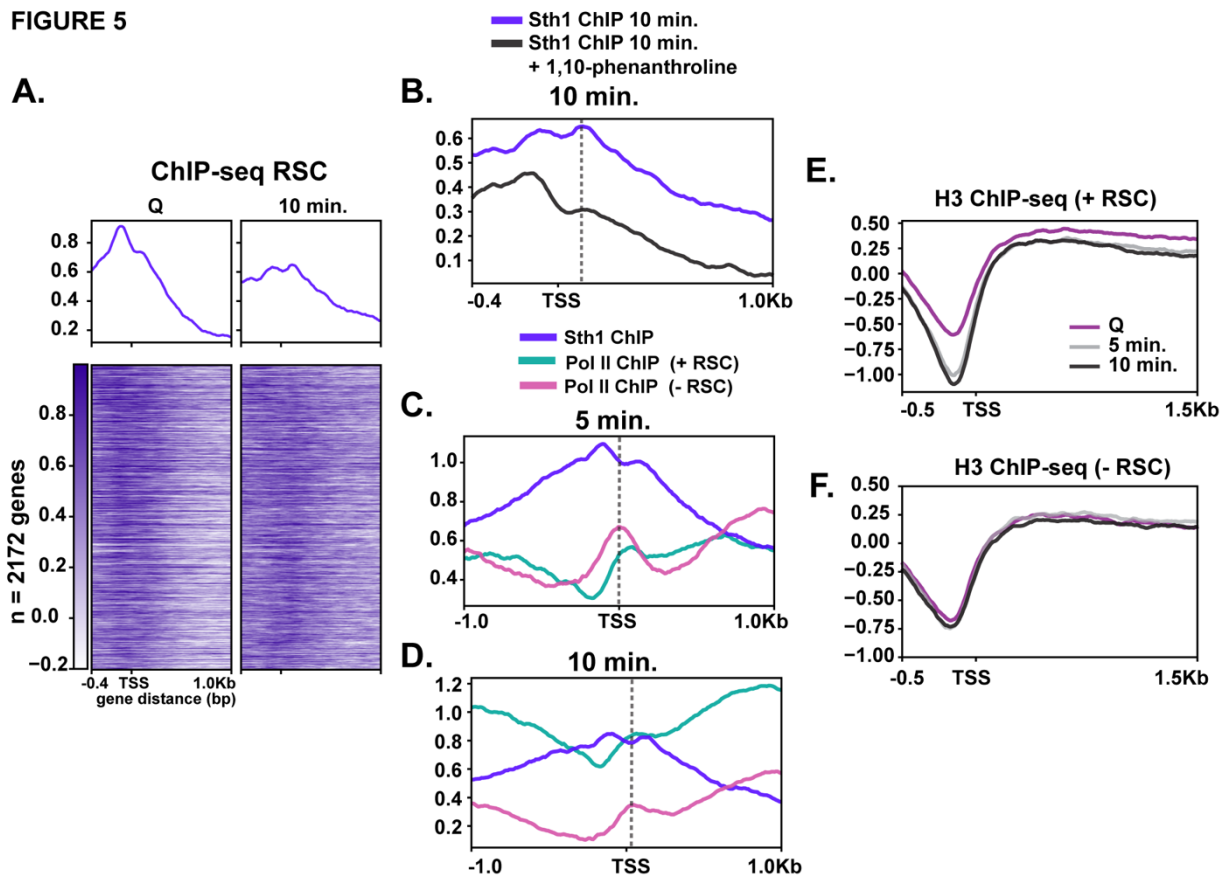

Figure 5. RSC depletion causes severe Pol II mislocalization defects during quiescence exit.
C) ChIP-seq of RSC in Q and 10-minute time points. Genes are linked. **(B)**. ChIP-seq of RSC at 10-minutes of exit in the presence and absence of the transcription inhibitor 1,10-phenanthroline. **(C, D)** ChIP-seq of RSC and Pol II during exit. **(E-F)** H3 ChIP-seq in quiescence and during exit in the presence and absence of RSC.

FIGURE 5—supplement 1

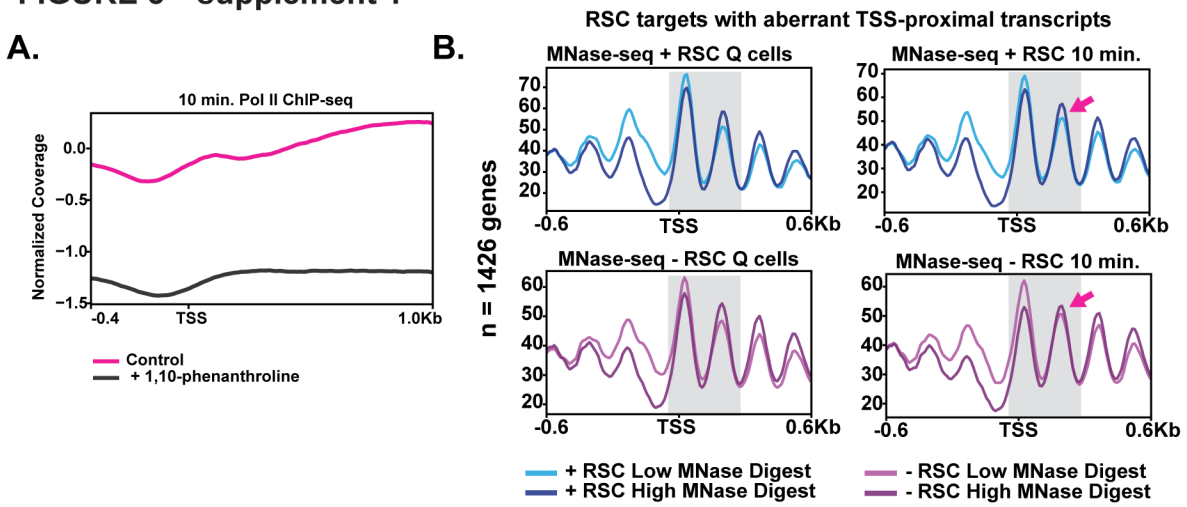

Figure 5—supplement 1

(A) ChIP-seq analysis of Pol II in the absence and presence of the transcription inhibitor 1,10-phenanthroline. **(B)** MNase-seq analysis assessing differences in MNase sensitivity in Q and ten-minutes for cells with and without RSC. The +2 nucleosome MNase-digestion differences are highlighted by the pink arrows.

FIGURE 6

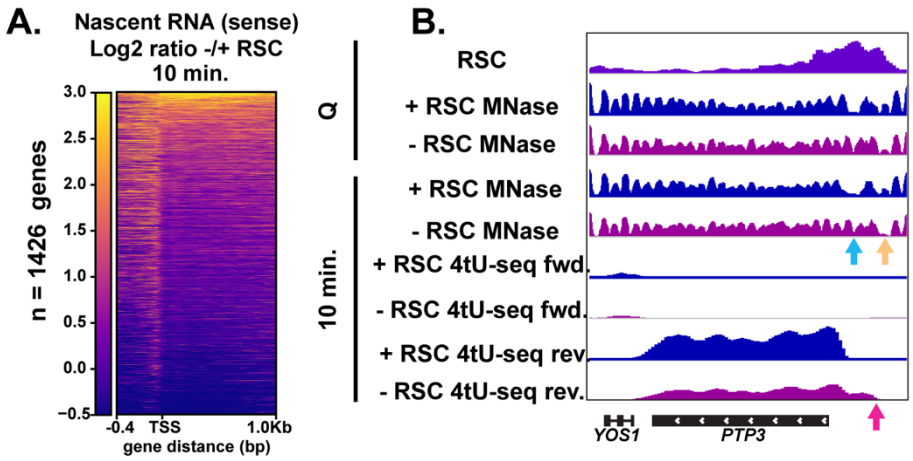

Figure 6. RSC depletion causes upstream transcription relative to canonical TSS
(A) Heatmap showing the Log_2 ratio of nascent sense transcripts in RSC-depleted versus non-depleted cells. Shown are 1426 genes that have upregulated transcripts at the 5'-ends of genes in the sense direction and have RSC ChIP signals. **(B)** Example gene of aberrant upstream transcript. Arrows direct to defects: blue arrow points to loss of NDR, yellow arrow points to gain of NDR, and pink arrow points to upstream RNA signal.

FIGURE 7

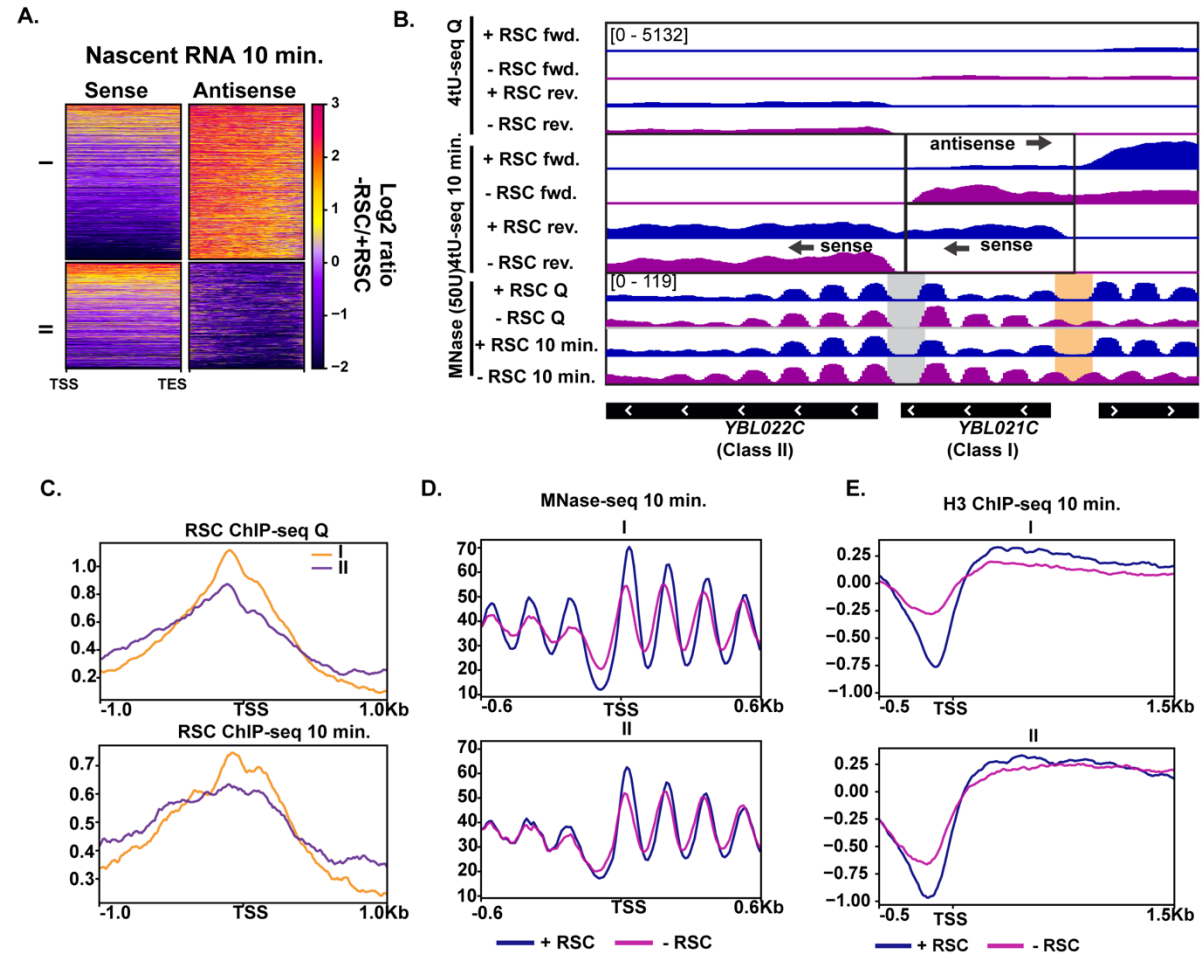

Figure 7. Aberrant antisense transcription arises when chromatin around sense transcripts is abrogated in the absence of RSC (A) Heatmaps of the Log_2 ratio of nascent RNAs that are RSC targets and give rise to antisense transcripts (cluster I, ~890 genes) when RSC is depleted and those where antisense transcripts are not made when the sense transcript NDR is unchanged (cluster II, ~600 genes). **(B)** Browser tracks of 4tU-seq and MNase-seq data. Boxes highlight defects (orange box) in NDRs and where antisense transcription arises from co-opted, intact NDRs (grey box). **(C)** ChIP-seq of RSC in quiescent cells and during exit at both cluster I and II. **(D)** MNase-seq at the 10-minute time point. (**E**.) 10-minute time point during exit of H3 ChIP-seq separated into the two clusters, I and II.

FIGURE 8

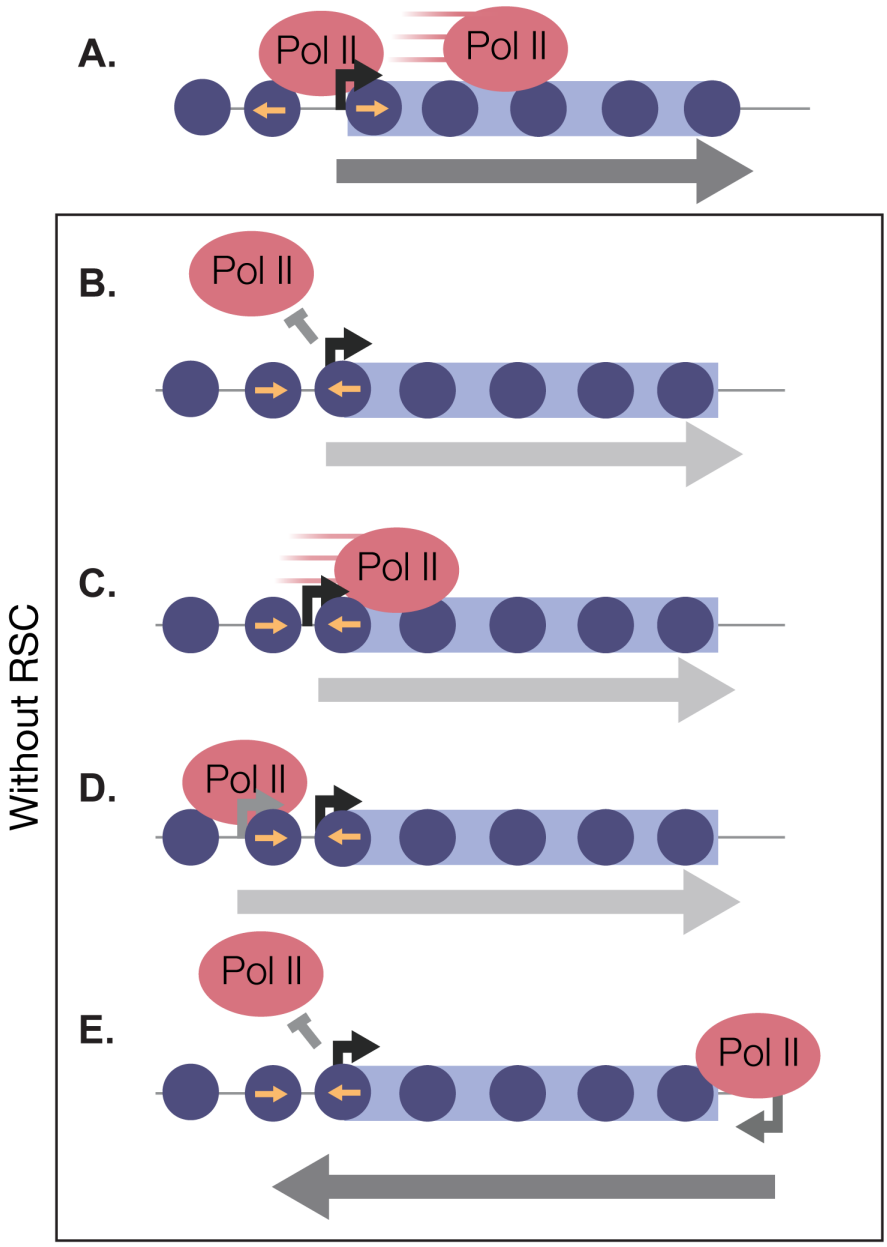

Figure 8. RSC safeguards the quiescent genome from aberrant transcription
In quiescent cells, RSC binds to NDRs upstream of Pol II transcribed genes. Upon quiescence exit, RSC shifts the +1 nucleosome to allow for Pol II occupancy and traverses into gene bodies **(A)**. In the absence of RSC NDRs are globally narrower and transcription initiation is blocked **(B).** At a subset of genes, RSC is required for efficient Pol II passage past the +1 nucleosome **(C)** and prevent upstream TSS selection **(D).** NDRs that are open despite RSC depletion become cryptic promoters and are utilized by transcription machinery to generate aberrant lncRNAs and antisense transcripts **(E)**.

References

1. Rando OJ, Winston F. Chromatin and Transcription in Yeast. Genetics. 2012;190: 351–387. doi:10.1534/genetics.111.132266

2. Sagot I, Laporte D. The cell biology of quiescent yeast – a diversity of individual scenarios. J Cell Sci. 2019;132: jcs213025. doi:10.1242/jcs.213025

3. Rittershaus ESC, Baek S-H, Sassetti CM. The Normalcy of Dormancy: Common Themes in Microbial Quiescence. Cell Host & Microbe. 2013;13: 643–651. doi:10.1016/j.chom.2013.05.012

4. Cheung TH, Rando TA. Molecular regulation of stem cell quiescence. Nat Rev Mol Cell Biol. 2013;14: 329–340. doi:10.1038/nrm3591

5. Tümpel S, Rudolph KL. Quiescence: Good and Bad of Stem Cell Aging. Trends in Cell Biology. 2019;29: 672–685. doi:10.1016/j.tcb.2019.05.002

6. McKnight JN, Boerma JW, Breeden LL, Tsukiyama T. Global Promoter Targeting of a Conserved Lysine Deacetylase for Transcriptional Shutoff during Quiescence Entry. Molecular Cell. 2015;59: 732–743. doi:10.1016/j.molcel.2015.07.014

7. Swygert SG, Kim S, Wu X, Fu T, Hsieh T-H, Rando OJ, et al. Condensin-Dependent Chromatin Compaction Represses Transcription Globally during Quiescence. Mol Cell. 2019;73: 533-546.e4. doi:10.1016/j.molcel.2018.11.020

8. Chapman NM, Boothby MR, Chi H. Metabolic coordination of T cell quiescence and activation. Nat Rev Immunol. 2020;20: 55–70. doi:10.1038/s41577-019-0203-y

9. Gray JV, Petsko GA, Johnston GC, Ringe D, Singer RA, Werner-Washburne M. “Sleeping Beauty”: Quiescence in Saccharomyces cerevisiae. MMBR. 2004;68: 187–206. doi:10.1128/MMBR.68.2.187-206.2004

10. Allen C, Büttner S, Aragon AD, Thomas JA, Meirelles O, Jaetao JE, et al. Isolation of quiescent and nonquiescent cells from yeast stationary-phase cultures. J Cell Biol. 2006;174: 89–100. doi:10.1083/jcb.200604072

11. Luger K, Mäder AW, Richmond RK, Sargent DF, Richmond TJ. Crystal structure of the nucleosome core particle at 2.8 Å resolution. Nature. 1997;389: 251–260. doi:10.1038/38444

12. Lorch Y, LaPointe JW, Kornberg RD. Nucleosomes inhibit the initiation of transcription but allow chain elongation with the displacement of histones. Cell. 1987;49: 203–210. doi:10.1016/0092-8674(87)90561-7

13. Hainer SJ, Kaplan CD. Specialized RSC: Substrate Specificities for a Conserved Chromatin Remodeler. BioEssays. 2020;42: 2000002. doi:10.1002/bies.202000002

14. Cairns BR, Lorch Y, Li Y, Zhang M, Lacomis L, Erdjument-Bromage H, et al. RSC, an Essential, Abundant Chromatin-Remodeling Complex. Cell. 1996;87: 1249–1260. doi:10.1016/S0092-8674(00)81820-6

15. Du J, Nasir I, Benton BK, Kladde MP, Laurent BC. Sth1p, a Saccharomyces cerevisiae Snf2p/Swi2p homolog, is an essential ATPase in RSC and differs from Snf/Swi in its interactions with histones and chromatin-associated proteins. Genetics. 1998;150: 987–1005.

16. Saha A. Chromatin remodeling by RSC involves ATP-dependent DNA translocation. Genes & Development. 2002;16: 2120–2134. doi:10.1101/gad.995002

17. Zofall M, Persinger J, Kassabov SR, Bartholomew B. Chromatin remodeling by ISW2 and SWI/SNF requires DNA translocation inside the nucleosome. Nat Struct Mol Biol. 2006;13: 339–346. doi:10.1038/nsmb1071

18. Kasten M, Szerlong H, Erdjument-Bromage H, Tempst P, Werner M, Cairns BR. Tandem bromodomains in the chromatin remodeler RSC recognize acetylated histone H3 Lys14. EMBO J. 2004;23: 1348–1359. doi:10.1038/sj.emboj.7600143

19. Angus-Hill ML, Schlichter A, Roberts D, Erdjument-Bromage H, Tempst P, Cairns BR. A Rsc3/Rsc30 Zinc Cluster Dimer Reveals Novel Roles for the Chromatin Remodeler RSC in Gene Expression and Cell Cycle Control. Molecular Cell. 2001;7: 741–751. doi:10.1016/S1097-2765(01)00219-2

20. Varela I, Tarpey P, Raine K, Huang D, Ong CK, Stephens P, et al. Exome sequencing identifies frequent mutation of the SWI/SNF complex gene PBRM1 in renal carcinoma. Nature. 2011;469: 539–542. doi:10.1038/nature09639

21. Kadoch C, Hargreaves DC, Hodges C, Elias L, Ho L, Ranish J, et al. Proteomic and bioinformatic analysis of mammalian SWI/SNF complexes identifies extensive roles in human malignancy. Nat Genet. 2013;45: 592–601. doi:10.1038/ng.2628

22. Badis G, Chan ET, van Bakel H, Pena-Castillo L, Tillo D, Tsui K, et al. A Library of Yeast Transcription Factor Motifs Reveals a Widespread Function for Rsc3 in Targeting Nucleosome Exclusion at Promoters. Molecular Cell. 2008;32: 878–887. doi:10.1016/j.molcel.2008.11.020

23. Hartley PD, Madhani HD. Mechanisms that Specify Promoter Nucleosome Location and Identity. Cell. 2009;137: 445–458. doi:10.1016/j.cell.2009.02.043

24. Prajapati HK, Ocampo J, Clark DJ. Interplay among ATP-Dependent Chromatin Remodelers Determines Chromatin Organisation in Yeast. Biology. 2020;9: 190. doi:10.3390/biology9080190

25. Kubik S, O'Duibhir E, de Jonge WJ, Mattarocci S, Albert B, Falcone J-L, et al. Sequence-Directed Action of RSC Remodeler and General Regulatory Factors Modulates +1 Nucleosome Position to Facilitate Transcription. Molecular Cell. 2018;71: 89-102.e5. doi:10.1016/j.molcel.2018.05.030

26. Ng HH. Genome-wide location and regulated recruitment of the RSC nucleosome-remodeling complex. Genes & Development. 2002;16: 806–819. doi:10.1101/gad.978902

27. Yen K, Vinayachandran V, Batta K, Koerber RT, Pugh BF. Genome-wide Nucleosome Specificity and Directionality of Chromatin Remodelers. Cell. 2012;149: 1461–1473. doi:10.1016/j.cell.2012.04.036

28. Ramachandran S, Zentner GE, Henikoff S. Asymmetric nucleosomes flank promoters in the budding yeast genome. Genome Res. 2015;25: 381–390. doi:10.1101/gr.182618.114

29. Soutourina J, Bordas-Le Floch V, Gendrel G, Flores A, Ducrot C, Dumay-Odelot H, et al. Rsc4 Connects the Chromatin Remodeler RSC to RNA Polymerases. MCB. 2006;26: 4920–4933. doi:10.1128/MCB.00415-06

30. Spain MM, Ansari SA, Pathak R, Palumbo MJ, Morse RH, Govind CK. The RSC Complex Localizes to Coding Sequences to Regulate Pol II and Histone Occupancy. Molecular Cell. 2014;56: 653–666. doi:10.1016/j.molcel.2014.10.002

31. Biernat E, Kinney J, Dunlap K, Rizza C, Govind CK. The RSC complex remodels nucleosomes in transcribed coding sequences and promotes transcription in *Saccharomyces cerevisiae*. Genomics; 2020 Mar. doi:10.1101/2020.03.11.987974

32. Xi Y, Yao J, Chen R, Li W, He X. Nucleosome fragility reveals novel functional states of chromatin and poises genes for activation. Genome Research. 2011;21: 718–724. doi:10.1101/gr.117101.110

33. Knight B, Kubik S, Ghosh B, Bruzzone MJ, Geertz M, Martin V, et al. Two distinct promoter architectures centered on dynamic nucleosomes control ribosomal protein gene transcription. Genes Dev. 2014;28: 1695–1709. doi:10.1101/gad.244434.114

34. Teif VB, Beshnova DA, Vainshtein Y, Marth C, Mallm J-P, Höfer T, et al. Nucleosome repositioning links DNA (de)methylation and differential CTCF binding during stem cell development. Genome Res. 2014;24: 1285–1295. doi:10.1101/gr.164418.113

35. Kubik S, Bruzzone MJ, Jacquet P, Falcone J-L, Rougemont J, Shore D. Nucleosome Stability Distinguishes Two Different Promoter Types at All Protein-Coding Genes in Yeast. Molecular Cell. 2015;60: 422–434. doi:10.1016/j.molcel.2015.10.002

36. Floer M, Wang X, Prabhu V, Berrozpe G, Narayan S, Spagna D, et al. A RSC/Nucleosome Complex Determines Chromatin Architecture and Facilitates Activator Binding. Cell. 2010;141: 407–418. doi:10.1016/j.cell.2010.03.048

37. Brahma S, Henikoff S. RSC-Associated Subnucleosomes Define MNase-Sensitive Promoters in Yeast. Molecular Cell. 2019;73: 238-249.e3. doi:10.1016/j.molcel.2018.10.046

38. Schlichter A, Kasten MM, Parnell TJ, Cairns BR. Specialization of the chromatin remodeler RSC to mobilize partially-unwrapped nucleosomes. eLife. 2020;9: e58130. doi:10.7554/eLife.58130

39. Percharde M, Bulut-Karslioglu A, Ramalho-Santos M. Hypertranscription in Development, Stem Cells, and Regeneration. Developmental Cell. 2017;40: 9–21. doi:10.1016/j.devcel.2016.11.010

40. Miller C, Schwalb B, Maier K, Schulz D, Dümcke S, Zacher B, et al. Dynamic transcriptome analysis measures rates of mRNA synthesis and decay in yeast. Mol Syst Biol. 2011;7: 458. doi:10.1038/msb.2010.112

41. Duffy EE, Rutenberg-Schoenberg M, Stark CD, Kitchen RR, Gerstein MB, Simon MD. Tracking Distinct RNA Populations Using Efficient and Reversible Covalent Chemistry. Molecular Cell. 2015;59: 858–866. doi:10.1016/j.molcel.2015.07.023

42. Radonjic M, Andrau J-C, Lijnzaad P, Kemmeren P, Kockelkorn TTJP, van Leenen D, et al. Genome-Wide Analyses Reveal RNA Polymerase II Located Upstream of Genes Poised for Rapid Response upon S. cerevisiae Stationary Phase Exit. Molecular Cell. 2005;18: 171–183. doi:10.1016/j.molcel.2005.03.010

43. Young CP, Hillyer C, Hokamp K, Fitzpatrick DJ, Konstantinov NK, Welty JS, et al. Distinct histone methylation and transcription profiles are established during the development of cellular quiescence in yeast. BMC Genomics. 2017;18: 107. doi:10.1186/s12864-017-3509-9

44. Martin BJE, Brind'Amour J, Kuzmin A, Jensen KN, Liu ZC, Lorincz M, et al. Transcription shapes genome-wide histone acetylation patterns. Nat Commun. 2021;12: 210. doi:10.1038/s41467-020-20543-z

45. Noe Gonzalez M, Blears D, Svejstrup JQ. Causes and consequences of RNA polymerase II stalling during transcript elongation. Nat Rev Mol Cell Biol. 2021;22: 3–21. doi:10.1038/s41580-020-00308-8

46. Churchman LS, Weissman JS. Nascent transcript sequencing visualizes transcription at nucleotide resolution. Nature. 2011;469: 368–373. doi:10.1038/nature09652

47. Hubert JC, Guyonvarch A, Kammerer B, Exinger F, Liljelund P, Lacroute F. Complete sequence of a eukaryotic regulatory gene. The EMBO Journal. 1983;2: 2071–2073. doi:10.1002/j.1460-2075.1983.tb01702.x

48. Vinayachandran V, Reja R, Rossi MJ, Park B, Rieber L, Mittal C, et al. Widespread and precise reprogramming of yeast protein–genome interactions in response to heat shock. Genome Res. 2018;28: 357–366. doi:10.1101/gr.226761.117

49. Parnell TJ, Huff JT, Cairns BR. RSC regulates nucleosome positioning at Pol II genes and density at Pol III genes. EMBO J. 2008;27: 100–110. doi:10.1038/sj.emboj.7601946

50. Mahapatra S, Dewari PS, Bhardwaj A, Bhargava P. Yeast H2A.Z, FACT complex and RSC regulate transcription of tRNA gene through differential dynamics of flanking nucleosomes. Nucleic Acids Research. 2011;39: 4023–4034. doi:10.1093/nar/gkq1286

51. Kumar Y, Bhargava P. A unique nucleosome arrangement, maintained actively by chromatin remodelers facilitates transcription of yeast tRNA genes. BMC Genomics. 2013;14: 402. doi:10.1186/1471-2164-14-402

52. Nishimura K, Kanemaki MT. Rapid Depletion of Budding Yeast Proteins via the Fusion of an Auxin-Inducible Degron (AID). Current Protocols in Cell Biology. 2014;64. doi:10.1002/0471143030.cb2009s64

53. Tsuchiya E, Uno M, Kiguchi A, Masuoka K, Kanemori Y, Okabe S, et al. The Saccharomyces cerevisiae NPS1 gene, a novel CDC gene which encodes a 160 kDa nuclear protein involved in G2 phase control. EMBO J. 1992;11: 4017–4026.

54. Kubik S, Bruzzone MJ, Challal D, Dreos R, Mattarocci S, Bucher P, et al. Opposing chromatin remodelers control transcription initiation frequency and start site selection. Nat Struct Mol Biol. 2019;26: 744–754. doi:10.1038/s41594-019-0273-3

55. Klein-Brill A, Joseph-Strauss D, Appleboim A, Friedman N. Dynamics of Chromatin and Transcription during Transient Depletion of the RSC Chromatin Remodeling Complex. Cell Reports. 2019;26: 279-292.e5. doi:10.1016/j.celrep.2018.12.020

56. Ocampo J, Chereji RV, Eriksson PR, Clark DJ. Contrasting roles of the RSC and ISW1/CHD1 chromatin remodelers in RNA polymerase II elongation and termination. Genome Res. 2019;29: 407–417. doi:10.1101/gr.242032.118

57. Spain MM, Braceros KCA, Tsukiyama T, Fred Hutchinson Cancer Research Center, Division of Basic Sciences. SWI/SNF coordinates transcriptional activation through Rpd3-mediated histone hypoacetylation during quiescence entry. Molecular Biology; 2018 Sep. doi:10.1101/426288

58. Poramba-Liyanage DW, Korthout T, Cucinotta CE, van Kruijsbergen I, van Welsem T, El Atmioui D, et al. Inhibition of transcription leads to rewiring of locus-specific chromatin proteomes. Genome Res. 2020;30: 635–646. doi:10.1101/gr.256255.119

59. Kireeva ML, Hancock B, Cremona GH, Walter W, Studitsky VM, Kashlev M. Nature of the Nucleosomal Barrier to RNA Polymerase II. Molecular Cell. 2005;18: 97–108. doi:10.1016/j.molcel.2005.02.027

60. Bondarenko VA, Steele LM, Újvári A, Gaykalova DA, Kulaeva OI, Polikanov YS, et al. Nucleosomes Can Form a Polar Barrier to Transcript Elongation by RNA Polymerase II. Molecular Cell. 2006;24: 469–479. doi:10.1016/j.molcel.2006.09.009

61. Lorch Y, Maier-Davis B, Kornberg RD. Histone Acetylation Inhibits RSC and Stabilizes the +1 Nucleosome. Molecular Cell. 2018;72: 594-600.e2. doi:10.1016/j.molcel.2018.09.030

62. Ye Y, Wu H, Chen K, Clapier CR, Verma N, Zhang W, et al. Structure of the RSC complex bound to the nucleosome. Science. 2019;366: 838–843. doi:10.1126/science.aay0033

63. Patel AB, Moore CM, Greber BJ, Luo J, Zukin SA, Ranish J, et al. Architecture of the chromatin remodeler RSC and insights into its nucleosome engagement. eLife. 2019;8: e54449. doi:10.7554/eLife.54449

64. Wagner FR, Dienemann C, Wang H, Stützer A, Tegunov D, Urlaub H, et al. Structure of SWI/SNF chromatin remodeller RSC bound to a nucleosome. Nature. 2020;579: 448–451. doi:10.1038/s41586-020-2088-0

65. Baker RW, Reimer JM, Carman PJ, Turegun B, Arakawa T, Dominguez R, et al. Structural insights into assembly and function of the RSC chromatin remodeling complex. Nat Struct Mol Biol. 2021;28: 71–80. doi:10.1038/s41594-020-00528-8

66. Shogren-Knaak M. Histone H4-K16 Acetylation Controls Chromatin Structure and Protein Interactions. Science. 2006;311: 844–847. doi:10.1126/science.1124000

67. Robinson PJJ, An W, Routh A, Martino F, Chapman L, Roeder RG, et al. 30 nm Chromatin Fibre Decompaction Requires both H4-K16 Acetylation and Linker Histone Eviction. Journal of Molecular Biology. 2008;381: 816–825. doi:10.1016/j.jmb.2008.04.050

68. Allahverdi A, Yang R, Korolev N, Fan Y, Davey CA, Liu C-F, et al. The effects of histone H4 tail acetylations on cation-induced chromatin folding and self-association. Nucleic Acids Research. 2011;39: 1680–1691. doi:10.1093/nar/gkq900

69. Swygert SG, Lin D, Portillo-Ledesma S, Lin P-Y, Hunt DR, Kao C-F, et al. Chromatin Fiber Folding Represses Transcription and Loop Extrusion in Quiescent Cells. Molecular Biology; 2020 Nov. doi:10.1101/2020.11.24.396713

70. Rawal Y, Chereji RV, Qiu H, Ananthakrishnan S, Govind CK, Clark DJ, et al. SWI/SNF and RSC cooperate to reposition and evict promoter nucleosomes at highly expressed genes in yeast. Genes Dev. 2018;32: 695–710. doi:10.1101/gad.312850.118

71. Han P, Chang C-P. Long non-coding RNA and chromatin remodeling. RNA Biology. 2015;12: 1094–1098. doi:10.1080/15476286.2015.1063770

72. Alcid EA, Tsukiyama T. ATP-dependent chromatin remodeling shapes the long noncoding RNA landscape. Genes Dev. 2014;28: 2348–2360. doi:10.1101/gad.250902.114

73. Gill JK, Maffioletti A, García-Molinero V, Stutz F, Soudet J. Fine Chromatin-Driven Mechanism of Transcription Interference by Antisense Noncoding Transcription. Cell Reports. 2020;31: 107612. doi:10.1016/j.celrep.2020.107612

74. Hainer SJ, Gu W, Carone BR, Landry BD, Rando OJ, Mello CC, et al. Suppression of pervasive noncoding transcription in embryonic stem cells by esBAF. Genes Dev. 2015;29: 362–378. doi:10.1101/gad.253534.114

75. Thomas BJ, Rothstein R. The genetic control of direct-repeat recombination in Saccharomyces: the effect of rad52 and rad1 on mitotic recombination at GAL10, a transcriptionally regulated gene. Genetics. 1989;123: 725–738.

76. Ausubel FM, B.R. Kingston RE, Moore DD, Seidman JG, Smith JA, Struhl K. Current Protocols in Molecular Biology. 1988; NYWiley-Interscience.

77. Cox JS, Chapman RE, Walter P. The unfolded protein response coordinates the production of endoplasmic reticulum protein and endoplasmic reticulum membrane. MBoC. 1997;8: 1805–1814. doi:10.1091/mbc.8.9.1805

78. Rodriguez J, McKnight JN, Tsukiyama T. Genome-Wide Analysis of Nucleosome Positions, Occupancy, and Accessibility in Yeast: Nucleosome Mapping, High-Resolution Histone ChIP, and NCAM. Current Protocols in Molecular Biology. 2014;108. doi:10.1002/0471142727.mb2128s108

79. Langmead B, Salzberg SL. Fast gapped-read alignment with Bowtie 2. Nat Methods. 2012;9: 357–359. doi:10.1038/nmeth.1923

80. Li H, Handsaker B, Wysoker A, Fennell T, Ruan J, Homer N, et al. The Sequence Alignment/Map format and SAMtools. Bioinformatics. 2009;25: 2078–2079. doi:10.1093/bioinformatics/btp352

81. Ramírez F, Dündar F, Diehl S, Grüning BA, Manke T. deepTools: a flexible platform for exploring deep-sequencing data. Nucleic Acids Research. 2014;42: W187–W191. doi:10.1093/nar/gku365

82. Xu Y, Bernecky C, Lee C-T, Maier KC, Schwalb B, Tegunov D, et al. Architecture of the RNA polymerase II-Paf1C-TFIIS transcription elongation complex. Nat Commun. 2017;8: 15741. doi:10.1038/ncomms15741

83. Bonnet J, Wang C-Y, Baptista T, Vincent SD, Hsiao W-C, Stierle M, et al. The SAGA coactivator complex acts on the whole transcribed genome and is required for RNA polymerase II transcription. Genes Dev. 2014;28: 1999–2012. doi:10.1101/gad.250225.114

84. Love MI, Huber W, Anders S. Moderated estimation of fold change and dispersion for RNA-seq data with DESeq2. Genome Biol. 2014;15: 550. doi:10.1186/s13059-014-0550-8